

# Formulation and evaluation of drug-loaded targeted magnetic microspheres for cancer therapy

Gerald G Enriquez<sup>1</sup>  
Syed AA Rizvi<sup>2</sup>  
Martin J D'Souza<sup>3</sup>  
Duc P Do<sup>1</sup>

<sup>1</sup>Department of Pharmaceutical Sciences, College of Pharmacy, Chicago State University, Chicago, IL, <sup>2</sup>Department of Pharmaceutical Sciences, College of Pharmacy, Nova Southeastern University, Fort Lauderdale, FL, <sup>3</sup>Department of Pharmaceutical Sciences, College of Pharmacy and Health Sciences, Mercer University, Atlanta, GA, USA

**Abstract:** Enhanced and targeted drug delivery using biodegradable microspheres is emerging as a promising approach for cancer therapy. The main objective of the present research was to formulate, characterize, and evaluate iron oxide (magnetic) containing a bovine serum albumin-based microsphere drug delivery system, capable of efficiently delivering sulforaphane, a histone deacetylase inhibitor, for an extended period of time in vivo. Magnetic microspheres were prepared by spray-drying and characterized for their physicochemical properties and dissolution profile. Further, they were evaluated for therapeutic efficacy in in vitro and in vivo systems. In vitro studies in B16 melanoma cells revealed that there was about 13%–16% more inhibition of cell viability when either 30  $\mu$ M or 50  $\mu$ M of sulforaphane was used with iron oxide in the polymeric carrier. Data from in vivo studies in C57BL/6 mice revealed that the magnetic microspheres (localized to the tumor site with the help of a strong magnet) inhibited 18% more tumor growth as compared with sulforaphane in solution. In addition, there was a 40% reduction in histone deacetylation levels in mice treated with iron oxide microspheres containing sulforaphane. Thus, magnetic microspheres are shown to be an effective drug delivery system for anticancer drugs.

**Keywords:** sulforaphane, delivery system, epigenetic therapy, microspheres, histone deacetylase inhibitor, iron oxide

## Introduction

In contrast with earlier investigations on understanding the genetic basis of disease, more recent efforts are directed towards deciphering the epigenetic events in abnormal function. Epigenetics refers to the study of heritable changes in gene expression without modifying the principal DNA sequence.<sup>1,2</sup> Epigenetic alterations play a profound role in the initiation and progression of cancer. At various stages of tumor progression, cells escape normal regulation of proliferation, differentiation, and cell death, leading to uncontrolled cell growth. This development results in abnormal activation of oncogenes and inactivation of tumor suppressor genes, which ultimately leads to cancer.<sup>3,4</sup> Identification of a number of key epigenetic events, including acetylation, phosphorylation, and methylation of histones during carcinogenesis has opened up avenues for using them as potential targets for potential epigenetic therapy. Hence, distinct from conventional therapies, epigenetic therapy has emerged as a promising approach for the treatment of cancer. Several therapeutic agents targeting epigenetic enzymes, such as deacetylases, have been explored and are being tested in clinical trials. Histone deacetylases (HDACs) are enzymes that are involved in the remodeling of chromatin. They play a critical role in the epigenetic regulation of gene expression.

Correspondence: Duc P Do  
Department of Pharmaceutical Sciences,  
College of Pharmacy, Chicago State  
University Chicago, IL 60628, USA  
Tel +1 773 821 2597  
Fax +1 773 821 2595  
Email ddo@csu.edu

Histone deacetylase inhibitors (HDACI) have come into view as a significant approach to reverse the epigenetic changes associated with cancer.<sup>5-7</sup> In addition, studies have shown that low doses of such agents are effective in changing aberrant epigenetic modifications.<sup>8,9</sup> Interestingly, the effects of epigenetic drugs (eg, histone deacetylase inhibitors) are known to be reversible.

Despite the promise of epigenetic therapy, a potential drawback of this approach is the activation of genes other than histones. In addition, many epigenetic agents are small molecular drugs; as a result, they face the same delivery problems as chemotherapeutic agents targeting cancer at the genetic level. Consequently, novel therapeutic agents and targeted delivery systems for cancer therapy are needed to reduce generalized toxicity and to increase the therapeutic effect.<sup>10-12</sup>

Magnetic targeted delivery systems have emerged as a promising strategy that can deliver therapeutic agents to the site of interest using an external magnetic field.<sup>13-18</sup> Magnetic microspheres injected into the body can be targeted to the disease site from the blood circulation using an effective external magnet. Studies have suggested that circulating drugs could reach disease sites at up to several-fold concentrations in comparison with administration of free drugs.<sup>19</sup> Further, these particles are known to be nontoxic, biocompatible, and injectable, and to accumulate at high levels in target tissue.<sup>20,21</sup>

Generally, targeted magnetic particles (micrometers to nanometers in size) contain a magnetic core and a polymer shell. The core contains small magnetic nanoparticles comprised of a magnetic agent, such as iron oxide (magnetite;  $\text{Fe}_3\text{O}_4$ ), nickel, cobalt, neodymium, iron, iron-boron, or samarium-cobalt. This component of the delivery system is responsible for the magnetic properties. The polymer shell surrounds the magnetic core and can protect the drug from degradation, reduce drug toxicity, and improve drug efficacy. Therapeutic agents are incorporated with a magnetic entity and polymers. Magnetic microspheres have been used as targeted delivery systems for interferon alpha-2b, protein drugs, 4'-epidoxorubin, doxorubicin, mitoxantrone, mitomycin C, etoposide, paclitaxel, and oxaliplatin.<sup>22,23</sup> In addition, magnetic delivery systems have been used to deliver radioisotopes. Hafeli et al showed that this delivery method improved tumor cell eradication without any harm to normal tissue.<sup>24</sup> Magnetic microspheres have also been investigated for other applications, such as hyperthermia therapy for cancer, gene therapy, contrast agents for magnetic resonance imaging, and for cell separation.<sup>25-27</sup>

This paper describes the second part of our investigation with albumin microspheres,<sup>28</sup> this time containing magnetic iron oxide as a possible targeted delivery vehicle for the epigenetic drug, sulforaphane (an HDACI). Melanoma is the cancer model used in this study because its incidence is rising worldwide, resulting in a global health issue.<sup>29</sup> Melanoma is the most deadly type of skin cancer, and is the leading cause of death from skin cancer. Sulforaphane is used as a model, and is a small molecule found in many green vegetables. Sulforaphane is a HDACI that has been shown to have anticancer properties via regulating the dynamics of acetylation/deacetylation.<sup>30</sup> Reversible acetylation of nuclear histones is a key component of gene regulation, and the ability of sulforaphane to target these acetylation mechanisms makes it an effective anticancer agent.<sup>31</sup> Development of iron oxide microspheres was an attempt to reduce the generalized toxicity of sulforaphane as well as to increase the therapeutic efficacy of the epigenetic agent. In addition, it has been shown that cancer cells take up microparticles more efficiently than solution.<sup>32</sup> This is due to high vascularization in the vicinity of cancer cells. Microspheres are taken up efficiently by macrophages,<sup>32,33</sup> which is an important phenomenon because macrophages are found abundantly near tumor sites.<sup>34</sup>

## Materials and methods

### Preparation of magnetic particles

Magnetic particles were prepared according to previously established and well optimized procedures,<sup>21</sup> with slight modifications as follows. Iron (II) chloride tetrahydrate and iron (III) chloride hexahydrate (Fisher Scientific, Pittsburgh, PA, USA) were dissolved in water to achieve final concentrations of 0.1 M. The aqueous solutions were mixed at a ratio of 1:2 for iron (II) and iron (III), respectively. Ammonium hydroxide (3 mL of 5 M) was added dropwise for one minute, followed by stirring for 20 minutes. The particles obtained were washed three times by ultracentrifugation for 30 minutes at  $15,000 \times g$  and  $10^\circ\text{C}$ .

### Preparation and formulation of magnetic microspheres

To formulate the magnetic microspheres, bovine serum albumin (Fisher Scientific) was dissolved in deionized water at a concentration of 1% w/v (previously optimized conditions<sup>28</sup>) and cross-linked chemically using glutaraldehyde for 24 hours at room temperature. Magnetic particles were added to the 1% crosslinked bovine serum albumin solution to achieve a desirable loading of magnetic particles. R,S-sulforaphane (LKT Laboratories Inc, St Paul, MN, USA) was

added to the suspension at the desired strength.<sup>28</sup> The solution was spray-dried (Mini Spray Dryer B-290, Büchi Analytical Inc, New Castle, DE, USA) using the following parameters: air flow rate, 800 NL per hour; pump feed rate, 1%; inlet temperature, 120°C; and outlet temperature, 60°C. Blank microspheres were obtained using the described procedure, but without addition of magnetic particles.

## Physical characterization of microspheres

The particle size, uniformity, and surface morphology of microsphere formulations were determined using scanning electron microscopy (JSM 5800LV, JEOL, Tokyo, Japan). Microspheres were coated with gold, and microscopic images were obtained. Further, a laser diffraction particle sizer (Zetasizer ZEN1600, Malvern, Westborough, MA, USA) was used to determine the particle size, size distribution, and zeta potential. Briefly, the microspheres were suspended in purified water at a concentration of 2 mg/mL. For particle size measurements, the median volume diameter of the microspheres was measured.

## Determination of iron oxide and drug content in magnetic microspheres

Determination of iron oxide was carried out based on a colorimetric assay adapted from Kalambur et al,<sup>35</sup> using the spectrophotometric detection of the complex formed after reaction of Fe<sup>2+</sup> with ferrozine. Iron oxide microspheres (10 mg) were weighed and dissolved in buffer A (50 mM Tris-HCl, pH 8.0, 10 mM EDTA) in a microcentrifuge tube. The microspheres were vortexed at regular intervals for two hours and incubated at 37°C. After two hours of incubation, buffer B (200 mM NaOH, 1% sodium dodecyl sulfate, 0.2 M ascorbic acid) was added to the microfuge tube and vortexed, followed by three hours of incubation at 37°C. After the incubation period, 0.2 mL of buffer containing 6.5 mM ferrozine, 13.1 mM neocuproine, 2 M ascorbic acid, and 5 M ammonium acetate was added and left for 30 minutes at room temperature. The absorbance was read at 562 nm in an ultraviolet-visible spectrophotometer (UV 2700, Shimadzu, Columbia, MD, USA). A standard curve was constructed using ferrous ammonium sulfate.

The amount of sulforaphane in the magnetic microspheres was determined by digesting the microspheres.<sup>28,36,37</sup> Briefly, 500 µL of buffer A (50 mM Tris-HCl, pH 8.0, 10 mM EDTA) was added to 10 mg of magnetic microspheres and vortexed at regular interval for 30 minutes. After two hours of incubation at room temperature, 500 µL of buffer B (200 mM NaOH, 1% sodium dodecyl sulfate, 0.2 M ascorbic acid) was added

to the suspension and vortexed. Next, 20 µL of proteinase K solution (10 mg/mL) was added to the suspension and incubated at 37°C for one hour. The suspension was then centrifuged at 14,000 × g for 10 minutes, and the supernatant was analyzed for drug content. Sulforaphane concentrations were measured using the ultraviolet-visible spectrophotometer at 235 nm. Encapsulation efficiency (or percent efficiency) was calculated by dividing the amount of drug inside magnetic microspheres by the theoretical weight of the drug before microencapsulation. Percent recovery was calculated by dividing the weight of the microspheres by the total initial weight of all components in the preparation.

## Drug release studies

In vitro release of sulforaphane from the microspheres was conducted in a modified USP type 1 water bath dissolution apparatus (Model 2500, Distek Inc, North Brunswick, NJ) at 37°C and 100 rpm, using phosphate-buffered solution (pH 7.4) as the medium. Twenty five milligrams of microspheres containing sulforaphane were placed in a dialysis bag (molecular weight cutoff 14 kDa) with 3 mL of phosphate-buffered solution (pH 7.4). At predetermined time points, 2 mL samples were removed and stored at 4°C until detection. After sampling, 2 mL of fresh phosphate-buffered solution (pH 7.4) was replaced to maintain the volume. Drug release was measured using the ultraviolet-visible spectrophotometer at 235 nm. Drug release studies were also conducted for blank microspheres used as the control.

## Cell culture studies

B16 melanoma cells were obtained from ATCC (Manassas, VA, USA) and cultured in RMPI-1640 medium containing 10% fetal bovine serum, 50 µg/mL penicillin, 50 U/mL streptomycin, and 2 mM L-glutamine at 37°C, in a humidified atmosphere of 95% air and 5% CO<sub>2</sub>. The medium was changed every other day. Melanoma cells were detached using 0.1% trypsin and 10 µM EDTA in phosphate-buffered solution.

## Uptake in cultured cells

Cellular uptake of sulforaphane was determined using the previously described procedures.<sup>28</sup> Briefly, confluent B16 cells were treated with fluorescamine-labeled iron oxide microspheres at a final concentration of 1 mg/mL. These microspheres were prepared according to the method described by Nettey et al.<sup>38</sup> At predetermined time points, the cells were washed twice with phosphate-buffered solution and lysed in lysis buffer (10 mM Tris-HCl, pH 8.0, 150 mM

NaCl, 1% Triton X-100). The cell lysate was then analyzed for fluorescamine using a fluorescent plate reader (Tecan, Morrisville, NC) with excitation 390 nm and emission 465 nm.

### Cytotoxicity of magnetic microspheres

Confluent cultures of B16 cells were dissociated, and the cells were seeded in 96-well plates for 24 hours. Iron oxide microspheres or sulforaphane-encapsulated iron oxide microspheres were added to cultures in the 96-well plates and incubated for 48 hours in the presence or absence of a magnetic field. Magnets (9000 gauss, Basic Wellness Store, Fairfield, FL, USA) were placed below some plates to evaluate the impact of a magnetic field on uptake of microspheres into the cells as compared with cultures not subjected to a magnetic field. Cytotoxicity was assessed using MTS assay (Promega, Fitchburg, WI, USA).

### In vitro internucleosomal DNA cleavage

After the tumor cells were treated with 30  $\mu\text{M}$  of R,S-sulforaphane for various time periods, the cells were harvested using trypsinization and washed with phosphate-buffered solution at 4°C. The cells were then suspended in lysis buffer (50 mM Tris-HCl, pH 8.0, 10 mM EDTA, and 0.5% sodium dodecyl sulfate) containing proteinase K 50  $\mu\text{g}/\text{mL}$  for three hours at 55°C. After incubation, samples were centrifuged at 14,000  $\times$  g for 10 minutes, and the supernatants were transferred to microcentrifuge tubes followed by phenol/chloroform/isoamyl alcohol (25:24:1) extraction. Two volumes of 100% ethanol were added to the supernatant to precipitate DNA, and this was followed by incubation at -20°C for at least one hour. DNA samples were centrifuged at 14,000  $\times$  g for 20 minutes. The samples were analyzed by electrophoresis in 1.2% agarose gel containing 0.2  $\mu\text{g}/\text{mL}$  ethidium bromide and visualized under ultraviolet illumination.

### In vivo studies

C57BL/6 mice were obtained from Charles River Laboratories (Wilmington, MA, USA). The animal protocols used were approved by the Institutional Animal Care and Use Committee at Mercer University, and the use and care of animals were performed in accordance with these guidelines. All mice were housed in a controlled environment and offered food and water ad libitum.

To induce tumors in C57BL/6 mice,  $2 \times 10^6$  B16 melanoma cells were suspended in RPMI-1640 medium and implanted subcutaneously between the ears of the mice. The skin was

gently lifted and a 22-gauge syringe containing 1 mL of melanoma cell suspension was inserted slightly below the skin layer. Melanoma cells were allowed to grow to form a tumor with an average volume of 100–200  $\text{mm}^3$ . The animals were randomly assigned to receive the vehicle control (RPMI-1640) or sulforaphane (500  $\mu\text{M}/\text{kg}$ ) via intraperitoneal injection three times a week for 28 days. There were four groups, ie, control, blank iron oxide microspheres, free sulforaphane solution, or sulforaphane-encapsulated iron oxide microspheres. Each group consisted of six mice. All treatments were administered intraperitoneally. The efficacy of the free sulforaphane solution and microsphere formulations was compared.

For antitumor activity, tumor volume was assessed using a vernier caliper. Tumor volumes were measured using the following formula:  $0.5 \times \text{length (mm)} \times \text{width (mm)} \times \text{width (mm)}$ . The mice were weighed twice a week. One-way analysis of variance was used to analyze the in vivo data.  $P < 0.05$  was considered to be statistically significant.

### Analysis of HDAC activity levels from tumor samples

Mouse tumor samples from all the groups were collected at day 28. Nuclear extracts were purified from mouse tumors as previously described.<sup>28</sup> They were stored at -80°C. Protein content was measured using a DC assay (Biorad, Hercules, CA, USA). HDAC activity was determined using the BioMol colorimetric HDAC activity assay kit according to the manufacturer's instructions (BioMol International, Farmingdale, NY, USA). Briefly, approximately 10  $\mu\text{g}$  of nuclear extract obtained from the mouse tumors was incubated with the HDAC assay buffer and colorimetric substrate for 30 minutes at 37°C. The lysine developer was then added. The sample was incubated at 37°C for 30 minutes and read in the enzyme-linked immunosorbent assay plate reader at 405 nm. The DC assay was used to determine protein content from nuclear extract samples.

## Results and discussion

### Physicochemical characterization of microspheres

Albumin microsphere formulations were prepared by spray-drying and characterized for zeta potential, average particle size, percent recovery, and percent encapsulation (Table 1). Albumin has been used extensively as a carrier to improve the pharmacokinetic profiles of therapeutic agents or to target a drug to the disease site.<sup>39</sup> Percent recovery was calculated for each microsphere formulation by dividing the weight of



**Table 1** Physicochemical characterization of microsphere formulations

Microsphere formulations	Zeta potential (mV)	Average particle size ( $\mu\text{m}$ )	Recovery (%)	Encapsulation (%)
Blank	$-32.6 \pm 1.7$	$2.0 \pm 0.1$	80	–
Iron oxide	$-34.8 \pm 1.4$	$2.1 \pm 0.3$	70	–
Sulforaphane	$-32.0 \pm 2.0$	$2.3 \pm 0.4$	75	80
Iron oxide and sulforaphane	$-32.9 \pm 1.8$	$2.4 \pm 0.5$	70	80

the microspheres by the total initial weight of all components in the suspension. Encapsulation (percent) efficiency was calculated by dividing the amount of drug inside the microspheres by the theoretical weight of the drug before microencapsulation. Based on our data, the encapsulation efficiency of the drug in iron oxide microspheres was 80%.

The microspheres were spherical and uniform in shape (Figure 1). This property is important because particles with a porous morphology can affect drug release, and this

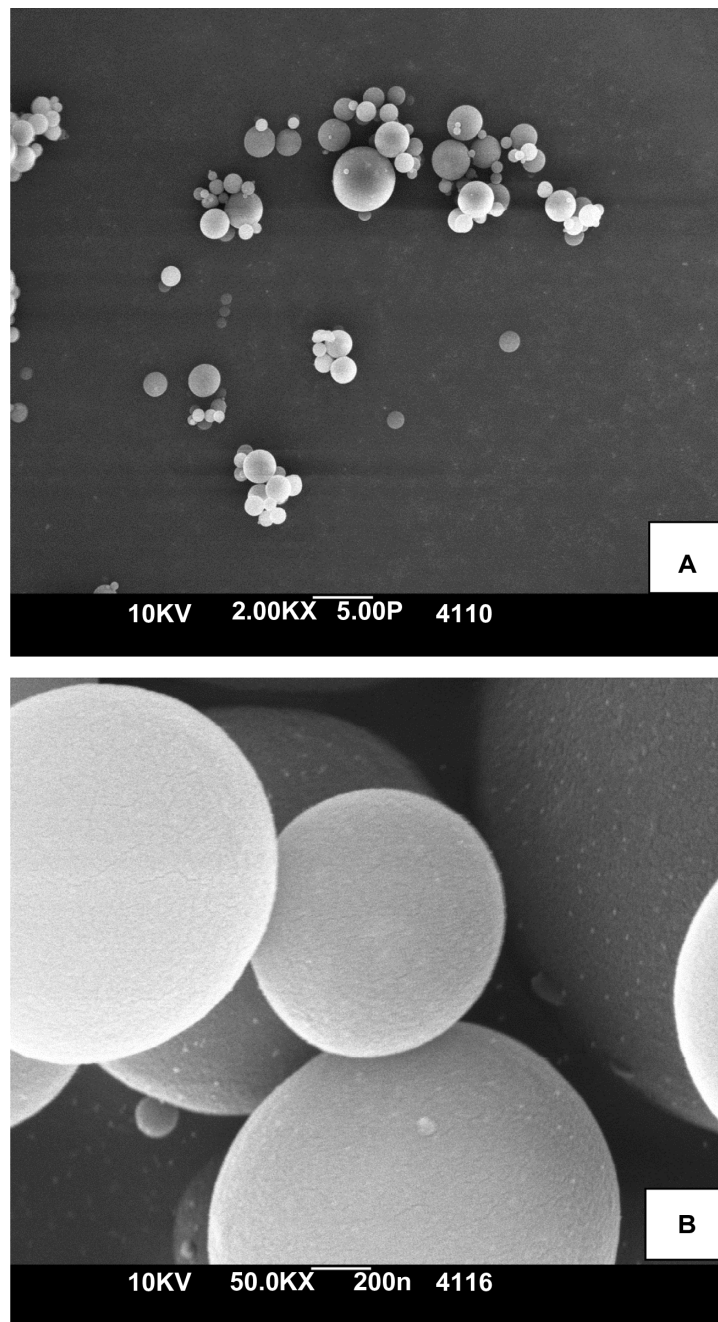


**Figure 1** Iron oxide microspheres. Representative scanning electron microscopic images of sulforaphane-encapsulated iron oxide microspheres. (A) 2,000 $\times$  magnification; (B) 50,000 $\times$  magnification.

changes the surface area of microspheres. The majority of microspheres in the groups were about 2  $\mu\text{m}$  in size. This size range is optimal for uptake by macrophages. Earlier studies have shown that microspheres 1–10  $\mu\text{m}$  in size are phagocytosed effectively by macrophages.<sup>40–42</sup>

The present research suggests that magnetic microspheres should be administered parenterally; as a result, determination of the stability of the microspheres in an injectable formulation is critical. When microspheres are in suspension, they may adhere to one another, forming aggregates. Such physical instability often poses a problem, given that aggregates are larger in size and tend to settle. The zeta potential is a physical property of a particle in suspension. The data show that the mean zeta potential for the microspheres was  $-32$  mV, indicating that these particles are stable when formulated into an injectable suspension formulation (because of interparticle repulsion resulting from same charge state).

## Uptake of microspheres in melanoma cells

The magnetic microspheres were labeled with fluorescamine according to the manufacturer's instructions. B16 melanoma cells were used for the uptake studies. The data indicate that there was a time-dependent increase in uptake of the microspheres in melanoma cells (Figure 2). At 24 hours, approximately 22% of the microspheres were taken up by the cells in the absence of a magnetic field.

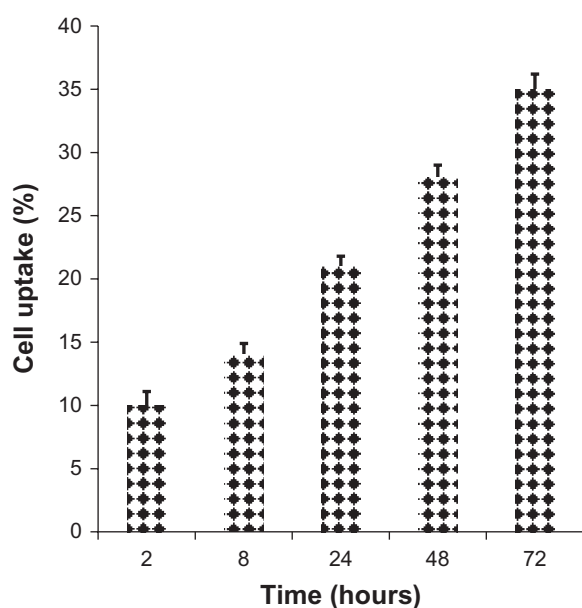


**Figure 2** Uptake of fluorescamine-labeled iron oxide microspheres in B16 melanoma cells.

**Notes:** Cell lysates were prepared and analyzed for the presence of fluorescamine. Data represent mean  $\pm$  SD ( $n = 4$ ). The experiments were repeated twice.

## Sulforaphane release from iron oxide microspheres

The release profile of sulforaphane from iron oxide microspheres was used to examine the behavior of microspheres formulated in solution. Standard curves were constructed to quantify the release of sulforaphane, which showed a small initial burst release effect, followed by a slow release phase (Figure 3A). It can be seen that 50% of the drug was released from the microspheres within 20 hours. The Higuchi plot (Figure 3B) shows that the microspheres released the drug in a sustained manner from solution.

## Cytotoxicity profile of cells treated with drug-loaded iron oxide microspheres

Our objective in using microspheres was to enhance the therapeutic effect of sulforaphane. In addition, we were interested in targeting drug-loaded iron oxide microspheres to the tumor for in vivo studies by applying a magnetic field near the tumor site. Targeted delivery systems reduce toxicity by localizing the anticancer drug to the disease site. In addition, more drug will accumulate within the tumor as opposed to being diluted in the systemic circulation. However, published reports also indicate that the carrier systems themselves are quite toxic in some cases.

Consequently, the toxicity of magnetic iron oxide microspheres was analyzed in cell culture prior to the in vivo studies using a colorimetric MTT assay at 490 nm. Our studies indicate that the magnetic microspheres were nontoxic, even at 20% of total concentration. This concentration of iron oxide was used for the in vivo studies (Figure 4).

We tested the in vitro efficacy of sulforaphane-loaded microspheres in cell culture. The data showed that, in the

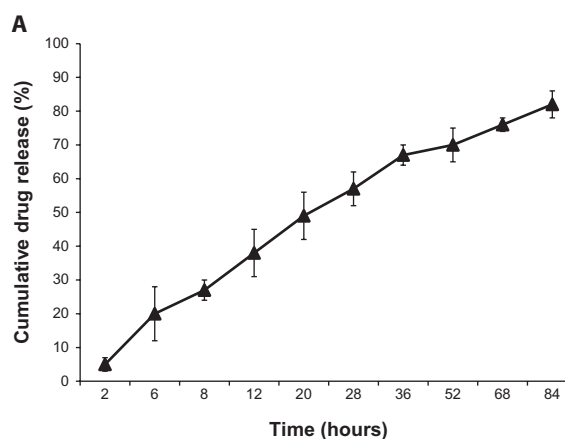


**Figure 3A** Release studies of sulforaphane.

**Note:** Sulforaphane concentrations were measured using a UV-Visible spectrophotometer at 235 nm.

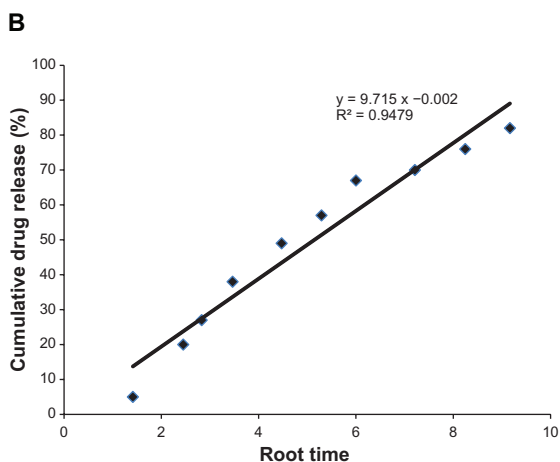


**Figure 3B** Higuchi analysis of sulforaphane from iron oxide microspheres.  
**Notes:** Higuchi analysis was carried out by plotting square root time against percent drug release. Sulforaphane concentrations were measured using a UV-Visible spectrophotometer at 235 nm.

presence of an external magnetic field, there was a higher toxicity profile when microspheres were loaded with magnetic iron oxide particles and sulforaphane, suggesting increased uptake of magnetic microspheres (Figure 4). In the presence of a magnetic field, there was about 13%–16% more inhibition of viability in B16 melanoma cells, when either 30 μM or 50 μM of sulforaphane was used with iron oxide in the polymeric carrier. The IC<sub>50</sub> for sulforaphane was 53.8 μM for B16 melanoma cells.

### DNA fragmentation in cells treated with sulforaphane-loaded iron oxide microspheres

Sulforaphane was microencapsulated in a biodegradable and biocompatible polymeric matrix to overcome some of

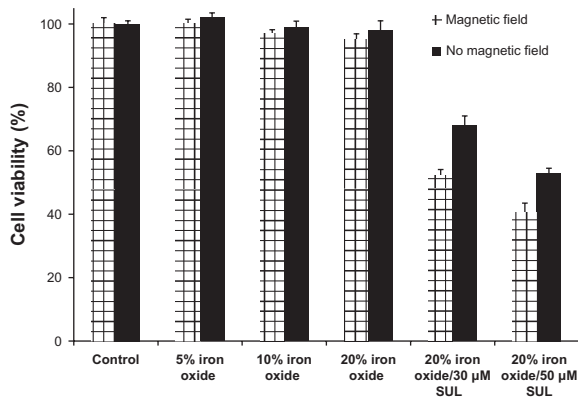


**Figure 4** Evaluation of the cytotoxicity of iron oxide microspheres and sulforaphane-encapsulated iron oxide microspheres on B16 melanoma cells in the presence and in the absence of a magnetic field.  
**Notes:** B16 cells were treated for 24 h. Cell viability was determined using an MTS assay. Data represent mean ± SD (n = 3). Each experiment was repeated two times.

the pharmacokinetic drawbacks of the drug, including its short half-life and high clearance. However, it is important to determine whether or not sulforaphane is stable in these microspheres after the spray-drying process and if sulforaphane in microspheres causes internucleosomal fragmentation. Our data indicate that in cells treated with R,S-sulforaphane solution and R,S-sulforaphane microspheres, a ladder of internucleosomal DNA fragments was observed, suggesting that iron oxide microspheres containing sulforaphane were as effective as the pure drug in an in vitro system (Figure 5).

### In vivo efficacy studies

The in vitro data for sulforaphane-loaded magnetic microspheres indicate that they exert similar cytotoxicity profiles as sulforaphane on cancer cells. Based on these promising in vitro data, in vivo efficacy studies were conducted in C57BL/6 mice. Experiments were performed to assess the efficacy of sulforaphane microspheres as a treatment for melanoma and to examine microspheres containing iron oxide as a delivery system targeted to the tumor site. Melanoma tumors were induced using B16 cells. Figure 6 summarizes

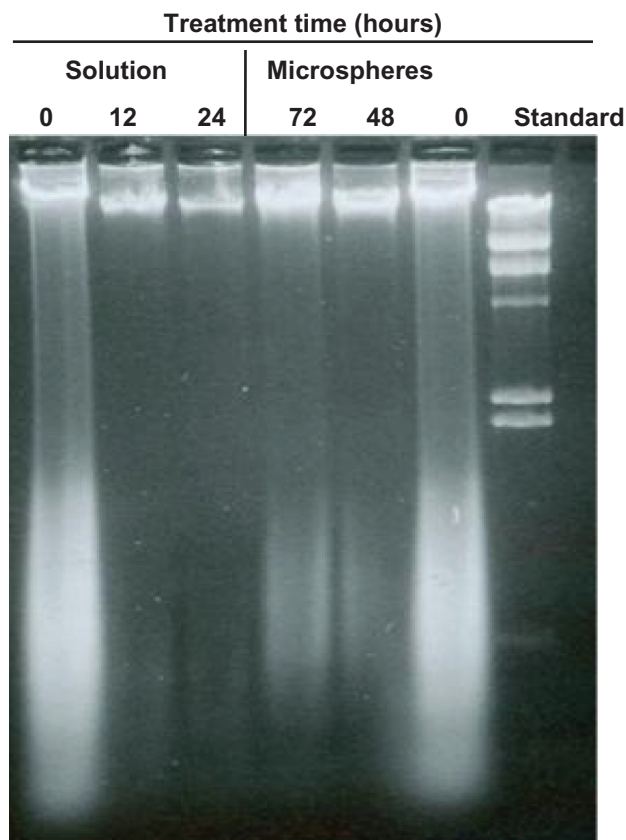


**Figure 5** Internucleosomal cleavage.  
**Notes:** DNA fragmentation in B16 cells with sulforaphane solution and sulforaphane encapsulated microspheres. Cells were treated with microspheres for 72 hours.

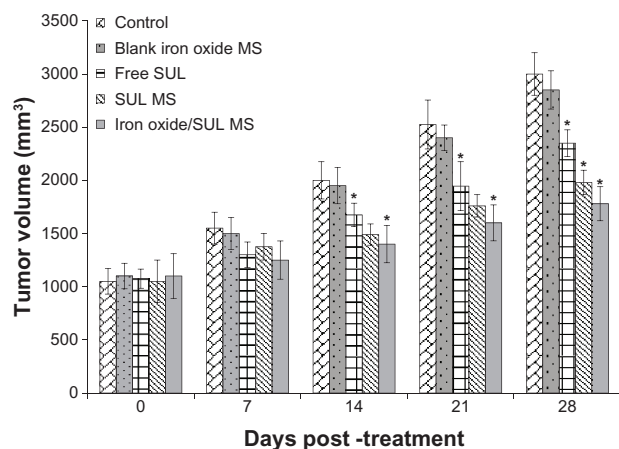


**Figure 6** In vivo antitumor efficacy of sulforaphane and sulforaphane-encapsulated iron oxide microspheres in C57BL/6 mice bearing B16 melanoma tumor.

**Notes:** Tumor volumes from the mice were determined until 28 days. Data represent mean  $\pm$  SD obtained from 6 animals treated per experimental group. \* $P < 0.05$  between free sulforaphane solution and sulforaphane-encapsulated microspheres.

the results of the in vivo efficacy studies using sulforaphane-loaded iron oxide microspheres. Mice bearing tumors were treated with iron oxide microspheres containing sulforaphane in the presence of an external magnetic field. The magnets were purchased from a commercial source (Basic Wellness Store) and were 9000 gauss in strength. Previous reports have indicated that magnets above 5000 gauss are effective for such use.<sup>43,44</sup> The mice were injected with the microsphere formulation and a magnet was placed near the tumor site. Sulforaphane-loaded iron oxide microspheres inhibited tumor growth more effectively than did the sulforaphane solution at weeks 2 and 3 after treatment (Figure 6). In addition, the sulforaphane microspheres inhibited approximately 15% more tumor growth as compared with the sulforaphane solution at week 4 following treatment.

In comparison with our previous studies of albumin microspheres encapsulating sulforaphane,<sup>28</sup> sulforaphane-loaded magnetic iron oxide microspheres increased the therapeutic efficacy by approximately 10%. Earlier studies reported in the literature using rats show that 72% of a single dose of the drug is recovered in urine within 24 hours.<sup>45,46</sup> Rapid clearance of sulforaphane from the body could explain the reduced inhibition of tumor growth in our studies when mice were treated with sulforaphane-loaded iron oxide microspheres and application of a magnetic field. The in vitro drug release data show that these magnetic microspheres released approximately 50% of the encapsulated drug within 20 hours. When the drug is released from the microspheres in vivo in mice, sulforaphane could be metabolized rapidly. To some extent, this could explain the marginal inhibitory effect

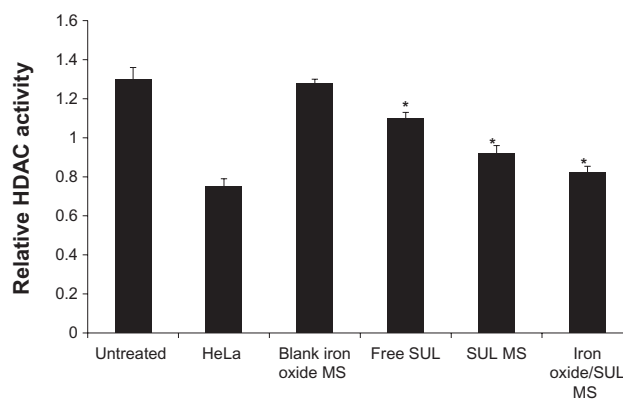


**Figure 7** Relative HDAC activity in mice melanoma tumors after treatment with sulforaphane and sulforaphane-encapsulated iron oxide microspheres.

**Notes:** Nuclear extracts were prepared from solid tumors and analyzed. Data represent mean  $\pm$  SD derived from 6 animals treated per experimental group in a single experiment. \* $P < 0.05$  between free sulforaphane solution and sulforaphane-encapsulated microspheres.

**Abbreviation:** HeLa, HeLa nuclear extract (positive control); MS, Microspheres; SUL, Sulforaphane; Untreated, Untreated mice (control).

(about 10%) on tumor growth as compared with sulforaphane microspheres not containing iron oxide in the formulation.

## HDAC activity levels from tumors of mice treated with HDACI

Histone deacetylase activity levels in tumor tissue were measured after treatment with the various microsphere formulations. Four weeks following treatment, the tumors were removed from the different groups of animals. Nuclear extracts were obtained from the tumors and analyzed for HDAC activity using a standard deacetylation curve. Figure 7 shows that there was a high level of HDAC activity in melanoma tumor tissue, which decreased when the mice were treated with sulforaphane microspheres or sulforaphane solution (by 40% and 18%, respectively). Previous reports in the literature show that HDAC activity is inhibited in mice treated with sulforaphane.<sup>47,48</sup>

## Conclusion

The present study demonstrates that sulforaphane exerts anticancer activity in melanoma cells in vitro. Inhibition of HDAC was also observed when the cells were treated with sulforaphane, suggesting that this is a potential mechanism of action, along with induction of apoptosis. Because of high clearance from the body and the instability of sulforaphane, albumin-based polymeric iron oxide formulations were developed in an attempt to improve the therapeutic effect. However, iron oxide microspheres are now shown to be an effective drug delivery system for anticancer drugs, particularly HDACIs. Similar results for the targeting effects of magnetic



drug delivery systems have been reported in the literature.<sup>49,50</sup> Downregulation of HDAC activity levels in melanoma tumors appears to be a novel approach to the treatment of cancer.

## Disclosure

The authors report no conflicts of interest.

## References

- Bird A. Perceptions of epigenetics. *Nature*. 2007;447(7143):396–398.
- Momparler RL. Cancer epigenetics. *Oncogene*. 2003; 22(42): 6479–6483.
- Gronbaek K, Hother C, Jones PA. Epigenetic changes in cancer. *APMIS*. 2007;115(10):1039–1059.
- Hanahan D, Weinberg RA. Hallmarks of cancer: the next generation. *Cell*. 2011;144(5):646–674.
- Bolden JE, Peart MJ, Johnstone RW. Anticancer activities of histone deacetylase inhibitors. *Nat Rev Drug Discov*. 2006;5(9):769–784.
- Butler JS, Koutelou E, Schibler AC, Dent SY. Histone-modifying enzymes: regulators of developmental decisions and drivers of human disease. *Epigenomics*. 2012;4(2):163–177.
- Popovic R, Licht JD. Emerging epigenetic targets and therapies in cancer medicine. *Cancer Discov*. 2012;2(5):405–413.
- Egger G, Liang G, Aparicio A, Jones PA. Epigenetics in human disease and prospects for epigenetic therapy. *Nature*. 2004;429(6990):457–463.
- Issa JP, Garcia-Manero G, Giles FJ, et al. Phase 1 study of low-dose prolonged exposure schedules of the hypomethylating agent 5-aza-2'-deoxycytidine (decitabine) in hematopoietic malignancies. *Blood*. 2004; 103(5):1635–1640.
- Chen X, Wang X, Wang Y, et al. Improved tumor-targeting drug delivery and therapeutic efficacy by cationic liposome modified with truncated bFGF peptide. *J Control Release*. 145(1):17–25.
- Mamot C, Drummond DC, Noble CO, et al. Epidermal growth factor receptor-targeted immunoliposomes significantly enhance the efficacy of multiple anticancer drugs in vivo. *Cancer Res*. 2005; 65(24):11631–11638.
- Wang X, Yang L, Chen ZG, Shin DM. Application of nanotechnology in cancer therapy and imaging. *CA Cancer J Clin*. 2008;58(2):97–110.
- Chen B, Wu W, Wang X. Magnetic iron oxide nanoparticles for tumor-targeted therapy. *Curr Cancer Drug Targets*. 2011;11(2): 184–189.
- Colombo M, Carregal-Romero S, Casula MF, et al. Biological applications of magnetic nanoparticles. *Chem Soc Rev*. 2012;41(11): 4306–4334.
- Jain S, Hirst DG, O'Sullivan JM. Gold nanoparticles as novel agents for cancer therapy. *Br J Radiol*. 2012;85(1010):101–113.
- Mikhaylov G, Vasiljeva O. Promising approaches in using magnetic nanoparticles in oncology. *Biol Chem*. 2011;392(11):955–960.
- Rosen JE, Chan L, Shieh DB, Gu FX. Iron oxide nanoparticles for targeted cancer imaging and diagnostics. *Nanomedicine*. 2012; 8(3):275–290.
- Tietze R, Lyer S, Durr S, Alexiou C. Nanoparticles for cancer therapy using magnetic forces. *Nanomedicine (Lond)*. 2012;7(3):447–457.
- Hafeli UO, Sweeney SM, Beresford BA, Humm JL, Macklis RM. Effective targeting of magnetic radioactive 90Y-microspheres to tumor cells by an externally applied magnetic field. Preliminary in vitro and in vivo results. *Nucl Med Biol*. 1995;22(2):147–155.
- Jain TK, Reddy MK, Morales MA, Leslie-Pelecky DL, Labhasetwar V. Biodistribution, clearance, and biocompatibility of iron oxide magnetic nanoparticles in rats. *Mol Pharm*. 2008;5(2):316–327.
- Jain TK, Morales MA, Sahoo SK, Leslie-Pelecky DL, Labhasetwar V. Iron oxide nanoparticles for sustained delivery of anticancer agents. *Mol Pharm*. 2005;2(3):194–205.
- Lubbe AS, Alexiou C, Bergemann C. Clinical applications of magnetic drug targeting. *J Surg Res*. 2001;95(2):200–206.
- Zhou S, Sun J, Sun L, et al. Preparation and characterization of interferon-loaded magnetic biodegradable microspheres. *J Biomed Mater Res B Appl Biomater*. 2008;87(1):189–196.
- Hafeli UO, Sweeney SM, Beresford BA, Sim EH, Macklis RM. Magnetically directed poly(lactic acid) 90Y-microspheres: novel agents for targeted intracavitary radiotherapy. *J Biomed Mater Res*. 1994; 28(8):901–908.
- Gazeau F, Levy M, Wilhelm C. Optimizing magnetic nanoparticle design for nanothermotherapy. *Nanomeicine (Lond)*. 2008;3(6):831–844.
- Hafeli UO. Magnetically modulated therapeutic systems. *Int J Pharm*. 2004;277(1–2):19–24.
- Lokwani P, Goyal A, Gupta S, Songara RK, Singh N, Rathore KS. Pharmaceutical applications of magnetic particles in drug delivery system. *Int J Pharm Res Dev*. 2011;3(7):147–156.
- Do DP, Pai SB, Rizvi SA, D'Souza MJ. Development of sulforaphane-encapsulated microspheres for cancer epigenetic therapy. *Int J Pharm*. 2010;386(1–2):114–121.
- Little EG, Eide MJ. Update on the current state of melanoma incidence. *Dermatol Clin*. 2012;30(3):355–361.
- Ho E, Clarke JD, Dashwood RH. Dietary sulforaphane, a histone deacetylase inhibitor for cancer prevention. *J Nutr*. 2009;139(12): 2393–2396.
- Myzak MC, Karplus PA, Chung FL, Dashwood RH. A novel mechanism of chemoprotection by sulforaphane: inhibition of histone deacetylase. *Cancer Res*. 2004;64(16):5767–5774.
- Oettinger CW, D'Souza MJ, Akhavein N, Peer GT, Taylor FB, Kinasewitz GT. Pro-inflammatory cytokine inhibition in the primate using microencapsulated antisense oligomers to NF-kappaB. *J Microencapsul*. 2007;24(4):337–348.
- Sharma A, Harper CM, Hammer L, Nair RE, Mathiowitz E, Egilmez NK. Characterization of cytokine-encapsulated controlled-release microsphere adjuvants. *Cancer Biother Radiopharm*. 2004; 19(6):764–769.
- Escribese MM, Sierra-Filardi E, Nieto C, et al. The prolyl hydroxylase PHD3 identifies proinflammatory macrophages and its expression is regulated by activin A. *J Immunol*. 2012;189(4):1946–1954.
- Kalambur VS, Longmire EK, Bischof JC. Cellular level loading and heating of superparamagnetic iron oxide nanoparticles. *Langmuir*. 2007;23(24):12329–12336.
- Bejugam NK, Uddin AN, Gayakwad SG, D'Souza MJ. Formulation and evaluation of albumin microspheres and its enteric coating using a spray-dryer. *J Microencapsul*. 2008;25(8):577–583.
- Gayakwad SG, Bejugam NK, Akhavein N, Uddin NA, Oettinger CE, D'Souza MJ. Formulation and in vitro characterization of spray-dried antisense oligonucleotide to NF-kappaB encapsulated albumin microspheres. *J Microencapsul*. 2009;26(8):692–700.
- Nettey H, Haswani D, D'Souza M, Oettinger C. In-vitro anti-microbial effect of encapsulated vancomycin on internalized *Staph. aureus* within endothelial cells. *Drug Dev Ind Pharm*. 2007;33(2):133–139.
- Elsadek B, Kratz F. Impact of albumin on drug delivery – new applications on the horizon. *J Control Release*. 2012;157(1):4–28.
- Ahsan F, Rivas IP, Khan MA, Torres Suarez AI. Targeting to macrophages: role of physicochemical properties of particulate carriers – liposomes and microspheres – on the phagocytosis by macrophages. *J Control Release*. 2002;79(1–3):29–40.
- Makino K, Nakajima T, Shikamura M, et al. Efficient intracellular delivery of rifampicin to alveolar macrophages using rifampicin-loaded PLGA microspheres: effects of molecular weight and composition of PLGA on release of rifampicin. *Colloids Surf B Biointerfaces*. 2004;36(1):35–42.
- Champion JA, Walker A, Mitragotri S. Role of particle size in phagocytosis of polymeric microspheres. *Pharm Res*. 2008;25(8): 1815–1821.
- Alexiou C, Jurgons R, Schmid RJ, et al. Magnetic drug targeting – biodistribution of the magnetic carrier and the chemotherapeutic agent mitoxantrone after locoregional cancer treatment. *J Drug Target*. 2003;11(3):139–149.

44. Nacev A, Beni C, Bruno O, Shapiro B. Magnetic nanoparticle transport within flowing blood and into surrounding tissue. *Nanomedicine (Lond)*. 2010;5(9):1459–1466.
45. Kassahun K, Davis M, Hu P, Martin B, Baillie T. Biotransformation of the naturally occurring isothiocyanate sulforaphane in the rat: identification of phase I metabolites and glutathione conjugates. *Chem Res Toxicol*. 1997;10(11):1228–1233.
46. Zhang Y, Munday R, Jobson HE, et al. Induction of GST and NQO1 in cultured bladder cells and in the urinary bladders of rats by an extract of broccoli (*Brassica oleracea italica*) sprouts. *J Agric Food Chem*. 2006;54(25):9370–9376.
47. Myzak MC, Dashwood WM, Orner GA, Ho E, Dashwood RH. Sulforaphane inhibits histone deacetylase in vivo and suppresses tumorigenesis in Apc-minus mice. *FASEB J*. 2006;20(3):506–508.
48. Pledge-Tracy A, Sobolewski MD, Davidson NE. Sulforaphane induces cell type-specific apoptosis in human breast cancer cell lines. *Mol Cancer Ther*. 2007;6(3):1013–1021.
49. Jia WJ, Liu JG, De Zhang Y, et al. Preparation, characterization, and optimization of pancreas-targeted 5-Fu loaded magnetic bovine serum albumin microspheres. *J Drug Target*. 2007;15(2):140–145.
50. Kang XJ, Dai YL, Ma PA, et al. Poly(acrylic acid)-modified Fe<sub>3</sub>O<sub>4</sub> microspheres for magnetic-targeted and pH-triggered anticancer drug delivery. *Chemistry*. 18(49):15676–15682.

### International Journal of Nanomedicine

## Publish your work in this journal

The International Journal of Nanomedicine is an international, peer-reviewed journal focusing on the application of nanotechnology in diagnostics, therapeutics, and drug delivery systems throughout the biomedical field. This journal is indexed on PubMed Central, MedLine, CAS, SciSearch®, Current Contents®/Clinical Medicine,

Submit your manuscript here: <http://www.dovepress.com/international-journal-of-nanomedicine-journal>

Dovepress

Journal Citation Reports/Science Edition, EMBase, Scopus and the Elsevier Bibliographic databases. The manuscript management system is completely online and includes a very quick and fair peer-review system, which is all easy to use. Visit <http://www.dovepress.com/testimonials.php> to read real quotes from published authors.